American Society for Precision Engineering 16th Annual Meeting, November 10-15, 2001, Crystal City, Virginia

KINEMATIC MODELING AND ANALYSIS OF A PLANAR MICRO-POSITIONER

Nicholas G. Dagalakis, John A. Kramar, Edward Amatucci, and Robert Bunch
National Institute of Standards and Technology, Gaithersburg, Maryland 20899

1. Introduction

The tremendous growth of opto-electronic devices manufacturing has raised the need for high performance micro-positioners, which are used in their assembly and alignment. The static and dynamic performance of micro-positioners depends in part on the quality of operation of their controllers, which in turn depends to a significant degree on the accuracy of the kinematic and dynamic mathematical models upon which they are based. The objective of this work was to evaluate the accuracy of two kinematic mathematical models of a planar X-Y micro-positioner under a variety of testing conditions.

A fully instrumented X-Y Parallel Cantilever Bi-axial Micro-Positioner[1] (PCBMP), was used for the tests (Fig. 1). The performance of the stage was evaluated by measuring the output motions as a function of input displacements over a two-dimensional grid of test positions. Second-order and linear kinematic models were developed through an examination of the stage geometry. The performance test data was used to identify the unknown parameters of the kinematic models using least-squares fitting algorithms. The accuracy of the fits was examined under the conditions of varying the number of input test data or adding white noise.

2. Stage Performance

The static performance of the stage was evaluated by examining its input and output displacements while moving it throughout its motion range of about 130
input actuators are servo-controlled based on built-in capacitance gage sensors, thus eliminating the typical piezoceramic effects of hysteresis, non-linearity, and creep.[2] At each test position, along with the input position commands and capacitance gage data, we also recorded six output data: the X and Y position of the output stage, measured by separate capacitance gages[3]; and the angular orientation of the output stage in all three angular axes, with a redundancy in yaw (rotation about the Z-axis). The angles were measured using two orthogonally placed, two-dimensional, high-resolution autocollimators, which tracked a cube reflector on the stage. A LabView[4] program was written to scan the stages and read the data. The entire array of data was swept multiple times over a period of several hours to verify repeatability and correct for drift.

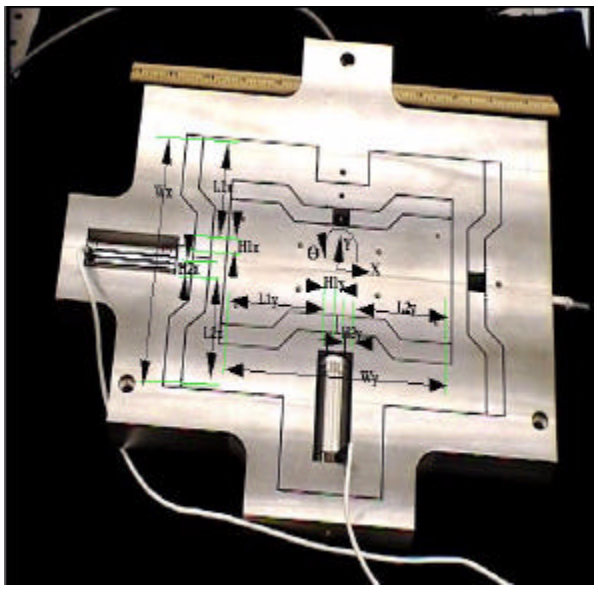

Fig. 1 Picture of a PCBMP stage with dimensions.

In initial tests, the motion actuators were coupled to the stage through a single universal joint (SUJ) on one end, the other end being hard mounted. The universal joint is a flexure device made from cross-bored pairs of holes to define the flexures and electron-discharge machined slots to release the motion. The sizes of the bores and their placements were optimized to achieve the required axial stiffness and lateral flexibility.[1] Later, since we had doubts about the ability of this coupling to

transmit pure axial loads, the tests were repeated with dual universal joint (DUJ) actuators, having flexure universal joint decoupling on both ends.

Fig. 2 shows plots of the angular stage errors as a function of position for the DUJ coupled stage. The maximum error is 0.1 arc seconds (0.5 microradians). The roughly periodic errors in the roll and yaw(2) measurements are auto-collimator noise, and are within specifications. That the error is not due to the stage is clearly evident by comparing with the yaw(1) measurements that were simultaneously acquired by the other autocollimator. These data demonstrate the exceptional absence of angular cross-talk in these stages.

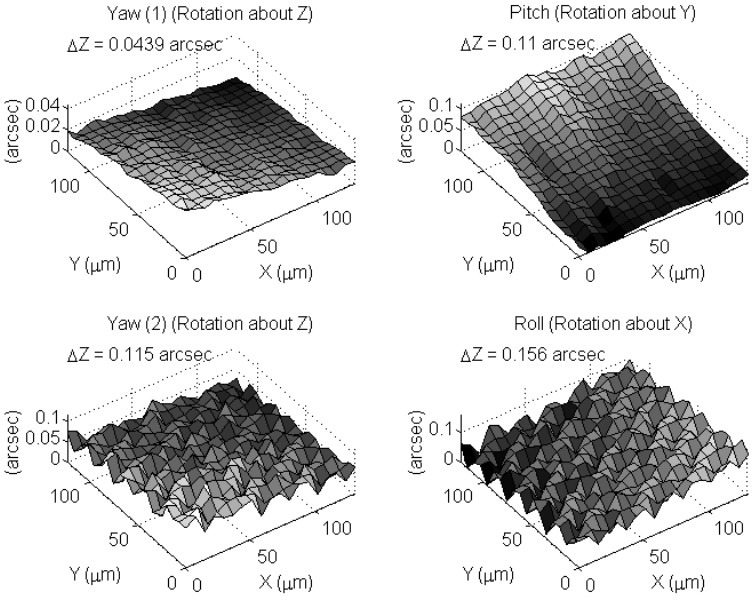

Fig. 2 Angular errors of the stage motion.

3. The Kinematic Model

The kinematic mathematical model equations are derived through an analysis of the stage geometry. Fig. 3 shows a schematic drawing of the stage. Only the Y-axis motion mechanism is shown for clarity. The input displacement is generated by the piezo-electric actuator (AC) and transmitted to the moving stage (MS) through flexures a_1 and a_2 of levers A_1 and A_2, respectively. These levers pivot about flexures b_1 and b_2, transmitting the actuator force to the moving stage through flexures c_1 and c_2. If not further constrained, due to the pivoting action, the attachment points of flexures c_1 and c_2 would generate arcuate motion. However, these arcs operate symmetrically on a rigid body. We therefore expect balanced elastic deformation, finally resulting in the approximate cancellation of the parasitic cross-axis motion. Levers A_{1t} and A_{2t} similarly constrain the other end of this stage of motion.

The approximate planar output motions as a function of the actuator inputs can be described by the following matrix equation:

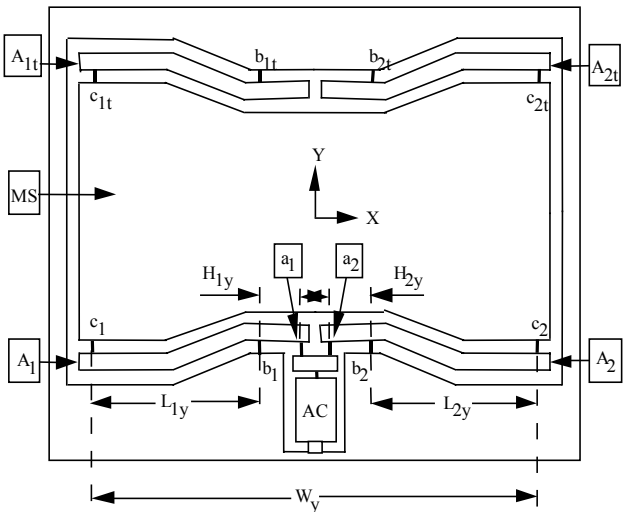

Fig. 3 Schematic drawing of the PCBMP Y-axis motion mechanism.

$$\begin{bmatrix} X_o \\ Y_o \\ \Theta_o \end{bmatrix} = \begin{bmatrix} \left(-\frac{L_{1x}}{2H_{1x}} - \frac{L_{2x}}{2H_{2x}}\right) & 0 & 0 & \left(-\frac{L_{1y}}{2H_{1y}^2} + \frac{L_{2y}}{2H_{2y}^2}\right) \\ 0 & \left(-\frac{L_{1y}}{2H_{1y}} - \frac{L_{2y}}{2H_{2y}}\right) & \left(-\frac{L_{1x}}{2H_{1x}^2} + \frac{L_{2x}}{2H_{2x}^2}\right) & 0 \\ \left(\frac{L_{1x}}{W_x H_{1x}} - \frac{L_{2x}}{W_x H_{2x}}\right) & \left(\frac{L_{1y}}{W_y H_{1y}} - \frac{L_{2y}}{W_y H_{2y}}\right) & 0 & 0 \end{bmatrix} \begin{bmatrix} X_i \\ Y_i \\ X_i^2 \\ Y_i^2 \end{bmatrix} . \qquad (1)$$

X_o, and Y_o, are the output stage motions in the X and Y axes and and Θ_o is the stage yaw. The parameter definitions can be gotten by reference to Fig. 3. Out of plane motion (Z_o) and rotations (pitch and roll) are ignored in this analysis. Eq. (1) includes first and second order terms in X_i and Y_i, which are the stage inputs generated by the actuators. In developing Eq. (1) we have assumed that certain nominally equal parameters, *e.g.* L_{1y} and L_{2y}, are in fact slightly different due to fabrication errors. The fabrication errors explicitly treated here are only a small subset of the possible errors. Other potential fabrication errors could be invoked which would result in additional terms, including terms where there are currently zeros in the matrix. On the other hand, for the first-order model, all the second order terms are forced to be zero.

The values of the kinematic model parameters were determined by first- or second-order fits in the X_i and Y_i input positions to the measured X_o and Y_o output positions and yaw of the stage. Six different least-squares techniques available in LabWindows CVI[5] were compared for curve-fitting. All the techniques generated similar results except for the "Square Root Free Givens Decomposition," which generated significantly worse fits. We define the accuracy of the fits as the root mean square difference between the modeled position and the measured position.

4. Variation of the Number of Test Data and the Amplitude of Sensor Noise

The identification of the kinematic model parameters was repeated four times with varying numbers of test data. Each time two columns of position test data located farthest from center and directed along the Y-axis were removed from the pool of data. These were the data where we would expect the largest amount of cross-talk error, since they involve the largest translation of the stage that carries the largest mass. Conversely, in typical applications, the central region would be the most used.

Fig. 4 shows a plot of the mathematical model evaluation error for the simple linear model (XY) and the second-order model (XY2). For each model the error is plotted for the case of SUJ and DUJ couplings. The more advanced model leaves smaller residual errors until the number of test data drops below approximately 65 to 75 (18% DUJ to 44% SUJ), at which point the situation is reversed. This raises questions that we will discuss in a future publication.

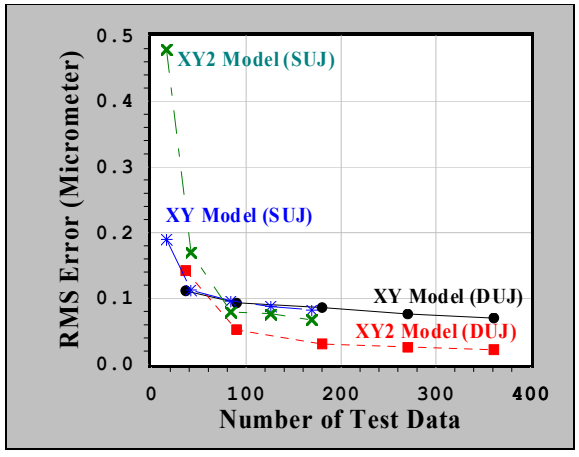

Fig. 4 Model error *vs*. the number of test data.

A possible explanation for this result is pointed to by an examination of the distribution of errors for the case of the linear model, using the complete set of test data, shown in Fig. 5. The highest magnitude of the errors appears to concentrate along a column at the end of travel of the X-axis actuator, near 60 micrometers. That is the region where we expect the maximum loading of the flexures, which can generate non-linearities. The linear model cannot describe these non-linearities, which now appear as errors. The removal of these

boundary regions from the pool of test data apparently hurts the advanced model more than the simple linear model. If the error plot of Fig. 5 is repeated for the case of the advanced model with the complete set of test data, the column of the high error region disappears, as well as the error droop in the central region. This will be explained in a future publication.

The plots of Fig. 4 also show that for the cases of the DUJ coupling, the errors tend to be lower than the for the SUJ coupling, *i.e.*, the mathematical models are in better agreement with the DUJ-coupling test data. One explanation for this is that the DUJ couplings come closer to satisfying the basic modeling assumption that the actuators exert a pure axial force.

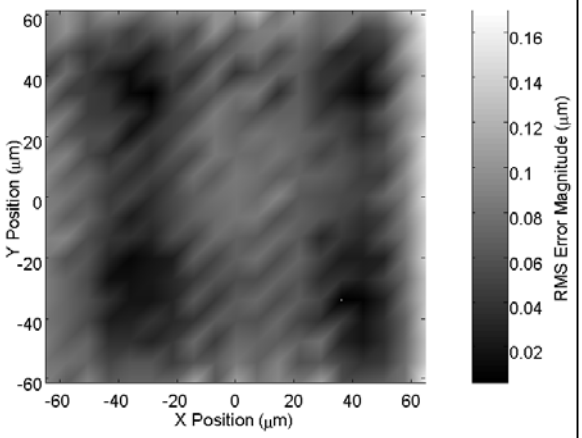

Fig. 5 Distribution of error after planar fit.

The effect of feedback sensor noise on the identification of the mathematical model parameters was also examined. This effect was simulated by adding white noise to the measured output displacements before solving for the kinematic model parameters. Arrays of random numbers that were uniformly distributed between the values of ± 2, ± 4, ± 6, ± 8 and ± 10 μm were used. The results show that the second-order model is more sensitive to sensor noise and generates higher estimation errors than those generated by the simple model for noise amplitudes exceeding approximately ± 1 μm. A possible reason for this result might be the sensitivity of the higher order terms of the advanced model to sensor noise.

5. Conclusions

The static performance for the stage using the DUJ coupling was significantly better than with the SUJ coupling, and the predictions of the mathematical models were also more accurate. It was found that the number of test locations plays a significant role in the accuracy of the kinematic model. The more advanced mathematical model is more accurate above a critical threshold for the number of test locations data used. Any further decrease results in significantly higher errors for the advanced model than for the simple model. It was found that the accuracy of both mathematical models decreases as the level of the noise increases. The more advanced model was more sensitive to noise, performing worse than the simple linear model, indicating that it should be used with caution and only when sufficiently good data is available.

6. Acknowledgements

This work was supported by the NIST Advance Technology Program, Office of Electronics and Photonics Technology.

7. References

[1] Amatucci E., Dagalakis N.G., Kramar J.A., Scire F.E., "Performance Evaluation of a Parallel Cantilever Biaxial Micropositioning Stage," ASPE 2000 Annual Meeting, Oct. 22-27, 2000, Scottsdale, Arizona.

[2] DPT actuators from Queensgate, Ltd. This and certain commercial products are identified in this paper to specify experimental procedures adequately. Such identification is not intended to imply recommendation or endorsement by the National Institute of Standards and Technology, nor is it intended to imply that the products identified are necessarily the best available for the purpose.

[3] ADE non-contact probes.

[4] LabView, National Instruments.

[5] LabWindows CVI, National Instruments.